Electronic structure of nanostructured ZnO from x-ray absorption and emission spectroscopy and the local density approximation

C. L. Dong,[1,2] C. Persson,[3] L. Vayssieres,[4] A. Augustsson,[1,5] T. Schmitt,[5] M. Mattesini,[5] R. Ahuja,[5] C. L. Chang,[2] and J.-H. Guo[1,*]

[1]*Advanced Light Source, Lawrence Berkeley National Laboratory, Berkeley, California 94720, USA*

[2]*Department of Physics, Tamkang University, Tamsui, Taiwan, Republic of China*

[3]*Department of Materials Science and Engineering, Royal Institute of Technology, SE-100 44 Stockholm, Sweden*

[4]*ICYS—National Institute of Materials Science, Namiki 1-1, Tsukuba, Ibaraki 305-0044, Japan*

[5]*Department of Physics, Uppsala University, Box 530, SE-751 21 Uppsala, Sweden*

(Received 26 March 2004; revised manuscript received 12 July 2004; published 18 November 2004)

O 1*s* absorption spectroscopy (XAS) and O $K\alpha$ emission spectroscopy (XES) were performed to study the electronic structure of nanostructured ZnO. The band gap is determined by the combined *absorption-emission* spectrum. Resonantly excited XES spectra showing an energy dependence in the spectral shape reveal the selected excitations to the different Zn 3*d*, 4*s*, and 4*p* states in hybridization with O 2*p* states. The partial density of state obtained from local density approximation (LDA) and LDA+*U* calculations are compared with the experimental results. The LDA+*U* approach is suitable to correct LDA self-interaction error of the cation *d* states. The atomic eigenstates of 3*d* in zinc and 2*p* in oxygen are energetically close, which induces the strong interaction between Zn 3*d* and O 2*p* states. This anomalous valence band cation-*d*–anion-*p* hybridization is verified by taking into account the strong localization of the Zn 3*d* states.

DOI: 10.1103/PhysRevB.70.195325 PACS number(s): 73.22.−f, 71.20.Nr, 71.15.Mb, 61.46.+w

ZnO is a wide-band-gap semiconductor, which has attracted a considerable attention during the past years due to its potential technological applications such as, for instance, high efficient vacuum fluorescent displays (VFD) and field-emission displays (FED).[1] ZnO has also been used for short-wavelength laser devices,[2] high power and high frequency electronic devices,[3] and light-emitting diodes (LED).[4] ZnO shows many advantages: (i) it has a larger exciton energy (~60 meV) than GaN (~23 meV) which is useful for efficient laser uv applications; (ii) the band gap is tunable from 2.8 to 3.3 eV and from 3.3 to 4 eV in the alloys with Cd and Mg, respectively;[5] (iii) wet chemical synthesis is possible; (iv) it has low power threshold at room temperature; (v) dilute Mn-doped ZnO shows room temperature ferromagnetism.[6] Recently, quantum size effects on the exciton and band-gap energies were observed in semiconductor nanocrystals.[7,8]

The controlled synthesis of ZnO nanostructures and an in-depth understanding of their chemical/physical properties and electronic structure are the key issues for the future development of ZnO based nanodevices. In this paper, we report on x-ray absorption (XAS) and x-ray emission spectroscopy (XES) experimental studies of nanostructured ZnO in zincite structure (wurtzite, $P6_3mc$) as well as the quantum calculation on periodic crystals.

The experiments were performed on beamline 7.0 at the Advanced Light Source. The beamline is equipped with a 99-pole, 5-cm period undulator and spherical grating monochromator.[9] The O 1*s* XAS spectra were obtained by measuring the photocurrent directly from the sample with the resolution set to 0.2 eV. The O *K* XES spectra were recorded by using the high-resolution grazing-incidence grating spectrometer with a two-dimensional detector.[10] The incidence angle of the incoming photon beam to the sample surface was about 30°. The resolution of the monochromator was set to 0.5 eV for 530-eV photon energy during XES measurement. The XES spectra were measured by using the 1200-lines/mm grating with a resolution of 0.3 eV. The size of ZnO nanoparticles was about 150 nm in diameter. Samples were prepared by hydrolysis of zinc salts in the presence of amine. The ZnO nanoparticles were precipitated by heating 0.1*M* zinc nitrate aqueous solution (*p*H 5) in the presence of 0.1*M* triethanolamine (TEA). The synthesis of ZnO nanoparticles was conducted in tightly stopper flasks, unstirred, at 100 °C for 24 h. The resulting suspension was then centrifuged. The precipitate was thoroughly washed with distilled water to remove any residual salt and dried at 100 °C. The synthesis and structural characterization of ZnO samples were reported in detail elsewhere.[11,12]

For over two decades, the electronic structure of ZnO was studied theoretically using the local density approximation (LDA). In the earlier LDA calculations the Zn 3*d* were treated as the core electrons,[13–16] which failed to predict the energy position of the 3*d* states. LDA calculations which treat the Zn 3*d* as valence states give a more reasonable valence-band structure, but then the Zn 3*d* states are energetically too high since the LDA does not accurately describe the self-interaction of the localized *d* states. Massidda *et al.*[17] have made a comparison between the Hartree-Fock, LDA, and the many-particle *GW* calculations. They found that the *GW* calculation lowers the Zn 3*d* states by about 1 eV compared to the LDA. Aryasetiawan and Gunnarsson[18] have shown that the *GW* calculation is capable of giving good electronic structure for both extended as well as rather localized semicore states. They also showed that even though the bandwidth of the *d* states may be very narrow, an atomic description of the energy *d* band is not sufficient. Therefore,

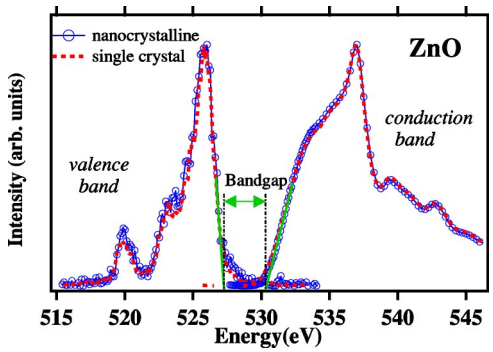

FIG. 1. Oxygen x-ray *absorption-emission* spectrum reflected conduction band and valence band near the Fermi level of ZnO nanoparticles in comparison with bulk ZnO.

an eigenvalue approach like the Slater transition state calculation (although derived from total energies) cannot describe satisfactorily the semicore like *d* states.

In this study, the calculations of the XES and XAS spectra were based on a full-potential linearized augmented plane wave method[19,20] with the LDA exchange-correlation of Perdew and Wang.[21] The Zn $3d^{10}4s^2$ and O $2s^22p^4$ orbitals are treated as valence states. Today's *GW* methods cannot produce a self-consistent potential, and we therefore correct the localization of the *d* states by means of the LDA$+U^{SIC}$,[20,22] i.e., the LDA with an on-site Coulomb potential for the cation *d* states. This self-interaction correction (SIC) has recently been shown to result in very accurate electronic and optical properties of various *s*-*p* hybridized semiconductors.[20,23] We consider U_d as a fitting parameter, choosing U_d(Zn)=6.0 eV that lowers the Γ-point Zn 3*d* states by 0.7–1.1 eV, in accordance with the *GW* results.[17] The different energy corrections of the Γ-point 3*d* states (i.e., 0.7–1.1 eV) are due to the change in the hybridization with O *p* states when the on-site correction potential is applied. In the simple picture, only the Zn 3*d* t_2-like states (and not the *e*-like states) couple with the O *p* states. The LDA$+U^{SIC}$ gives a more narrow band width of the Zn 3*d* states compared to the LDA method. The calculated O *K* XES and XAS spectra were obtained from the density of states (DOS) and the matrix elements of the dipole allowed transitions. We used the modified tetrahedron **k**-space integration method and a Lorentzian broadening of 0.6 eV.[19] The relatively large **k** mesh of 76 **k** points in the irreducible Brillouin zone is required to ensure convergence of the low-energy dipole-allowed transitions, since both the conduction-band minimum and the valence-band maximum are very nonparabolic near the Γ point. This is, however, less critical in the LDA $+U^{SIC}$ calculation than in the LDA calculation because the LDA$+U^{SIC}$ method yields normally improved band curvatures with more parabolic energy dispersion.[20]

The XES spectra of bulk and nanotructured ZnO are displayed together with the corresponding XAS spectrum in Fig. 1. The O *K* emission spectrum reflects the O 2*p* occupied states (valence band), and the O 1*s* absorption spectrum reflects the O 2*p* unoccupied states (conduction band). In the photon energy region of ~530–539 eV, the x-ray absorption can be mainly assigned to the O 2*p* hybridized with Zn 4*s*

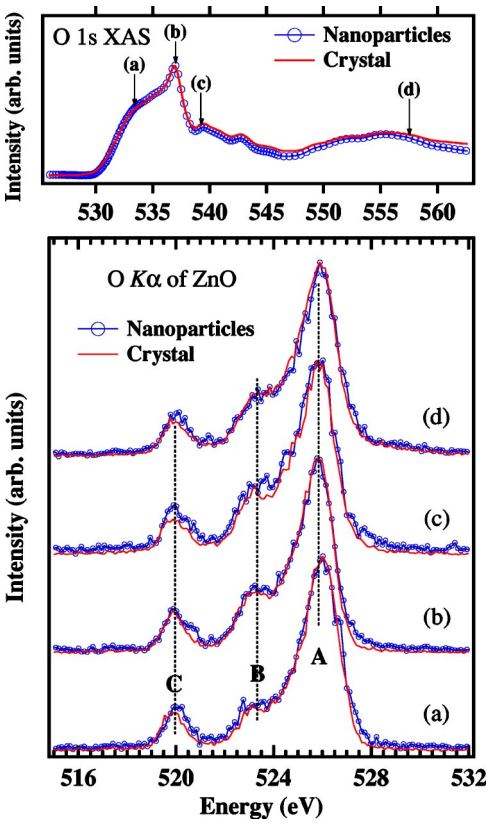

FIG. 2. A comparison of x-ray emission spectra of nanostructured and bulk crystalline ZnO recorded at selected excitation energies of (a), (b), (c), and (d) which are indicated in the XAS spectra (upper panel).

states. In the region of ~539–550 eV the spectrum is mainly attributed to O 2*p* hybridized with Zn 4*p* states. Above 550 eV, the contribution is mainly coming from O 2*p*–Zn 4*d* mixed states.[24] Stronger *s*-*p*-*d* hybridization was revealed in nanostructured ZnO since the contributions of features at 520 eV and 523 eV are enhanced. A well-defined band gap can be observed between the valence-band maximum and conduction-band minimum. Our *absorption-emission* spectrum yields the fundamental band-gap energy of 3.3 eV, which is in agreement with the 3.4 eV found for bulk ZnO.[25]

The O *K* emission spectra of ZnO bulk and nanoparticles, recorded at different excitation energies, are displayed in Fig. 2. The selected excitation energies are indicated in the XAS spectrum (inset in Fig. 2). By selecting different excitation energies, predominant contribution of specific admixture of unoccupied O 2*p* with Zn 3*d*, 4*s*, and 4*p* states is expected. Indeed, three distinct structures can be observed in the XES spectra, labeled as *A*, *B*, and *C*. Feature *A*, located at ~526 eV, is mainly due to O 2*p*–Zn 4*p* states. The low-energy shoulder (feature *B*) in 522–524 eV region arises from the mixed states of O 2*p*–Zn 4*s*. The single-band shape at 520 eV is attributed mainly to the O 2*p* hybridized with Zn 3*d* states. These assignments are in accordance with the previous photoemission valence band data.[26,27]

All spectra in Fig. 2 show the similar spectral profile at different excitation energies. However, there are changes in

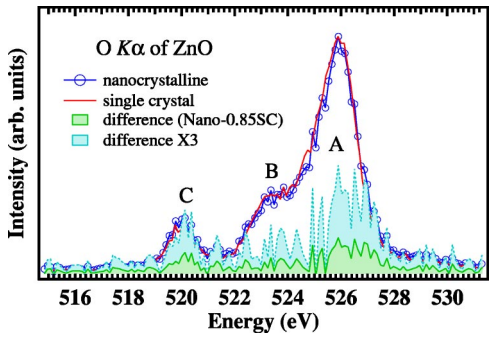

FIG. 3. The difference spectrum obtained, based on the variation of bulk and nanoparticles ZnO, from the spectra (d) in Fig. 2.

the intensity distribution for the three main emission features. The most intense feature *A* is found to shift about 0.2 eV towards higher energy in the spectrum (a) compared to the spectrum (b), which is opposite to the decrease of excitation energy. Such a shift may indicate that the oxygen atoms are on slightly inequivalent sites. Resonantly excited O *K*-emission spectra can reveal the difference between the inequivalent oxygen sites as we observed previously in the high-T_c superconductors.[28,29] The small intensity variations of spectral profile depend on the excitation energies, i.e., the changes for the ratios of the emission features B/A and C/A, may be attributed to the selected excitations to the conduction band in different symmetries, such as *s*, *p*, and *d* states. Feature *B* is enhanced as the excitation photon energy increases. Feature *B* has the highest intensity when the excitation energy is set to 537 eV, which corresponds to x-ray absorption prompting the 1*s* electron to the unoccupied O $2p-$Zn $4s$ mixing states in the conduction band, and consequently the x-ray emission from the occupied states (valence band) with the O $2p-$Zn $4s$ symmetry is enhanced. Feature *C* in nanostructured ZnO presented in spectra (c) and (d) are enhanced compared with bulk, which is attributed to stronger *p-d* hybridization observed in nanostructured ZnO. The spectral results show small but significant differences between spectra.

In order to emphasize the differences of spectra, the spectrum of bulk with no symmetry selectivity [i.e., spectrum (d)] has been subtracted from the spectrum of nanostructured ZnO by using a weighting factor, as shown in Fig. 3. The weighting factor was chosen by subtracting the maximal bulk spectrum without getting negative intensity as far as possible. The difference spectrum was then multiplied by factor of 3. Feature *C* has pronounced intensity compared to features *A* and *B*, which can be correlated to enhanced *p-d* hybridization in nanostructured ZnO.

The partial density of states (DOS) from and LDA as well as LDA^{SIC} calculation are displayed in Fig. 4. Both O $2p$ and Zn $3d$ wave functions are strongly localized and the O $2p$ states are very energetically close to the Zn $3d$ states, which implies a significantly strong interaction between O $2p$ and Zn $3d$ in ZnO. The energy gap of ZnO is primarily a result of the O $2p-$Zn $4s$ interaction, which shifts the O *p*–like states downwards and the Zn *s*–like states upwards. The O $2p$

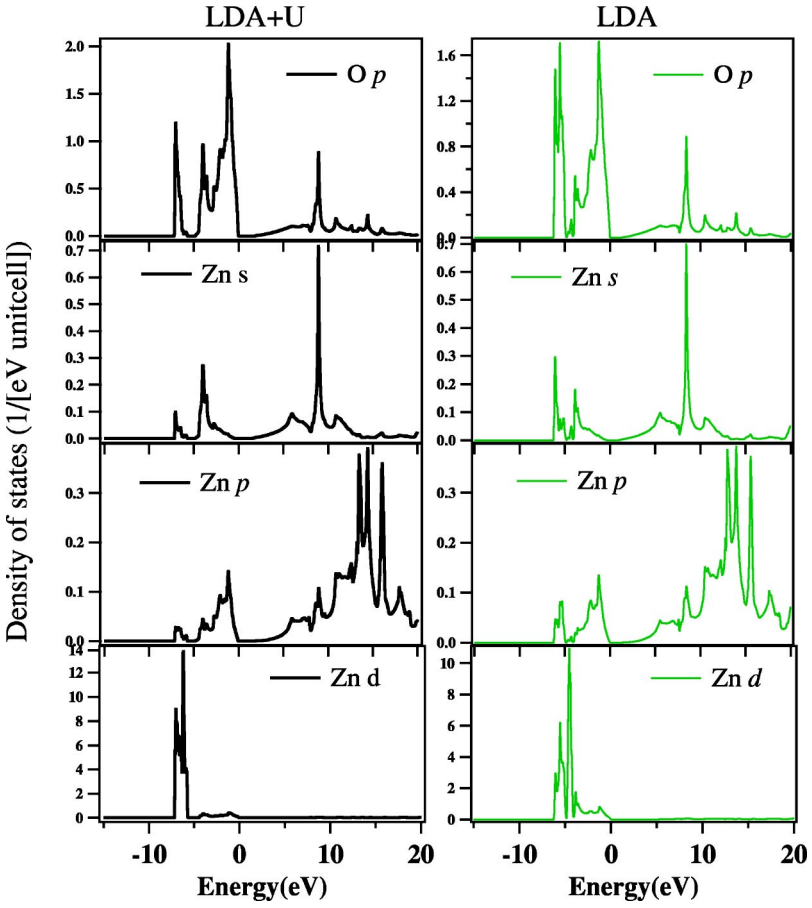

FIG. 4. The partial density of states from LDA and LDA+U^{SIC} calculations where the O $2p$, Zn $4p$, $4s$, and $3d$ bands are shown.

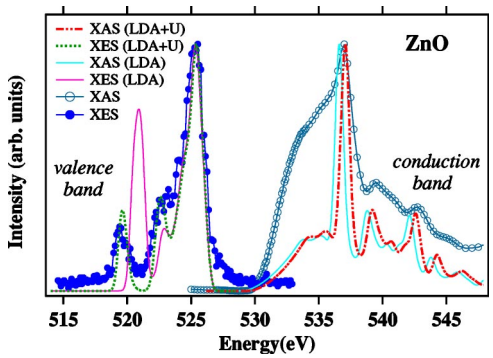

FIG. 5. Calculated O $K\alpha$ emission and absorption, performed within the LDA and methods, in comparison with experimental results.

states are thus shifted even closer to the Zn 3*d* levels. Therefore, strong *p*-*d* hybridization is expected in ZnO. In addition, the calculated LDA show nearly no energy gap between Zn 4*s* and Zn 3*d* state. The calculated LDA+U^{SIC} exhibits the clear energy gap at between −5 and −6 eV in the valence band. Thus, by comparing with the calculations and experiments, the locations of Zn 3*d* energy states can be reproduced fairly well by employing LDA+U^{SIC} calculation.

The O $K\alpha$ emission of the valence band (in Fig. 5) shows that the Zn 3*d*−O 2*p* mixed states lie about 7 eV below the valence-band maximum. The calculated XES spectrum from LDA gives 1.5-eV higher energy for the emission feature *C* in comparison with the measurement. The discrepancy was explained in term of an electronic relaxation in highly correlated electron systems.[30–32] However, the main reason for the discrepancy is related to LDA shortcoming of describing localized states. With the LDA+U^{SIC} approach, the Zn 3*d* states shift to the lower energy in the calculated XES spectrum. The emission features of *A*, *B*, and *C* are now in good agreement with the experimental spectrum. The correction of the Zn 3*d* states thus affects directly the O 2*p*. This is due to the strong valence band *p*-*d* hybridization, which is normally not seen for III-V and II-VI semiconductors.[23] Thus, by lowering the cation *d* states in ZnO, the valence band anion *p* states are lowered. Consequently, the LDA+U^{SIC} shows an energy gap between −5 and −6 eV where no O 1*s*-2*p* transitions are allowed. LDA shows no such energy gap. Thus, LDA produces an incorrect description of both the Zn 3*d* and O 2*p* valence-band electronic structures. This disagreement between the measured XES and the calculated LDA DOS was also noticed by McGuinness *et al.*[33]

In conclusion, the character of conduction band and valence band in ZnO nanoparticles was investigated. The band-gap energy of 3.3 eV is obtained from the *absorption-emission* spectrum. The resonantly excited O *K*-emission spectra show the energy dependence due to the selected excitations to the Zn different 3*d*, 4*s*, and 4*p* in hybridization with O 2*p* states. The partial density of states obtained from LDA and LDA+U^{SIC} calculations are compared with the experimental results. We find that the LDA+U^{SIC} approach is suitable to correct the LDA self-interaction error of the cation *d* states. With this on-site Coulomb correction potential, the Zn 3*d* states are lowered by ~1.0−1.5 eV, which results in a shift of the *p*-*d* hybridized O 2*p* states to the lower-energy region. Also, the strong valence band *p*-*d* hybridization is revealed in ZnO.

The Advanced Light Source is supported by the Director, Office of Science, Office of Basic Energy Sciences, Materials Sciences Division, of the U.S. Department of Energy under Contract No. DE-AC03-76SF00098 at Lawrence Berkeley National Laboratory. This work is also supported by the Swedish Research Council (VR).

*Author to whom correspondence should be addressed. Email address: jguo@lbl.gov

[1] S. Shionoya and W. M. Yen (eds.), *Phosphor Handbook* (CRC Press, Boca Raton, 1999), p. 255; C. X. Xu and X. W. Sun, Int. J. Nanotechnol. **1**, 452 (2004).
[2] J. E. Nause, III-Vs Review **12**, 28 (1999); S. S. Mao, Int. J. Nanotechnol. **1**, 42 (2004).
[3] M. W. Shin and R. J. Trew, Electron. Lett. **31**, 489 (1995).
[4] F. Hamdani, A. E. Botchkarev, H. Tang, W. Kim, and H. Morkoc, Appl. Phys. Lett. **71**, 3111 (1997); T. Detchprohm, K. Hiramatsu, H. Amano, and I. Akasaki, *ibid.* **61**, 2688 (1992).
[5] R. D. Vispute, V. Talyansky, S. Choopun, R. P. Sharma, T. Venkatesan, M. He, X. Tang, J. B. Halpern, M. G. Spencer, Y. X. Li, L. G. Salamanca-Riba, A. A. Iliadis, and K. A. Jones, Appl. Phys. Lett. **73**, 348 (1998); A. Ohtomo, M. Kawasaki, T. Koida, H. Koinuma, T. Sakurai, Y. Yoshida, M. Sumiya, S. Fuke, T. Yasuda, and Y. Segawa, Mater. Sci. Forum **264**, 1463 (1998).
[6] P. Sharma, A. Gupta, K. V. Rao, F. J. Owens, R. Sharma, R. Ahuja, J. M. Osorio Guillen, B. Johansson, and G. A. Gehring, Nat. Mater. **2**, 673 (2003).
[7] T. van Buuren, L. N. Dinh, L. L. Chase, W. J. Siekhaus, and L. J. Terminello, Phys. Rev. Lett. **80**, 3803 (1998).
[8] Y. K. Chang, H. H. Hsieh, W. F. Pong, M.-H. Tsai, F. Z. Chien, P. K. Tseng, L. C. Chen, T. Y. Wang, K. H. Chen, D. M. Bhusari, J. R. Yang, and S. T. Lin, Phys. Rev. Lett. **82**, 5377 (1999).
[9] T. Warwick, P. Heimann, D. Mossessian, W. McKinney, and H. Padmore, Rev. Sci. Instrum. **66**, 2037 (1995).
[10] J. Nordgren, G. Bray, S. Cramm, R. Nyholm, J.-E. Rubensson, and N. Wassdahl, Rev. Sci. Instrum. **60**, 1690 (1989).
[11] K. Keis, L. Vayssieres, H. Rensmo, S-E. Lindquist, and A. Hagfeldt, J. Electrochem. Soc. **148**, 149 (2001).
[12] K. Keis, L. Vayssieres, S-E. Lindquist, and A. Hagfeldt, Nanostruct. Mater. **12**, 487 (1999).
[13] S. Bloom and I. Ortenburger, Phys. Status Solidi B **58**, 561 (1973).
[14] J. R. Chelikowsky, Solid State Commun. **22**, 351 (1977).
[15] I. Ivanov and J. Pollmann, Phys. Rev. B **24**, 7275 (1981).
[16] D. H. Lee and J. D. Joannopoulos, Phys. Rev. B **24**, 6899 (1981).
[17] S. Massidda, R. Resta, M. Posternak, and A. Baldereschi, Phys. Rev. B **52**, 16 977 (1995).

[18] F. Aryasetiawan and O. Gunnarsson, Phys. Rev. B **54**, 17 564 (1996).
[19] P. Blaha, K. Schwarz, G. K. H. Madsen, D. Kvasnicka, and J. Luitz, *WIEN2k, An Augmented Plane Wave+Local Orbitals Program for Calculating Crystal Properties* (Karlheinz Schwarz, Techn. Univ. Wien, Austria, 2001).
[20] C. Persson and S. Mirbt (unpublished).
[21] J. P. Perdew and Y. Wang, Phys. Rev. B **45**, 13 244 (1992).
[22] V. I. Anisimov, I. V. Solovyev, M. A. Korotin, M. T. Czyzyk, and G. A. Sawatzky, Phys. Rev. B **48**, 16 929 (1993); A. I. Liechtenstein, V. I. Anisimov, and J. Zaanen, *ibid.* **52**, R5467 (1995); P. Novák, F. Boucher, P. Gressier, P. Blaha, and K. Schwarz, *ibid.* **63**, 235114 (2001).
[23] C. Persson and A. Zunger, Phys. Rev. B **68**, 073205 (2003).
[24] J.-H. Guo, L. Vayssieres, C. Persson, R. Ahuja, B. Johansson, and J. Nordgren, J. Phys.: Condens. Matter **14**, 6969 (2002).
[25] M. Huang, S. Mao, H. Feick, H. Yan, Y. Wu, H. Kind, E. Weber, R. Russo, and P. Yang, Science **292**, 1897 (2001).
[26] J. J. Yeh and I. Lindau, At. Data Nucl. Data Tables **32**, 1 (1985).
[27] R. T. Girard, O. Tjernberg, G. Chiaia, S. Söderholm, U. O. Karlsson, C. Wigren, H. Nylén, and I. Lindau, Surf. Sci. **373**, 409 (1997).
[28] J.-H. Guo, S. M. Butorin, N. Wassdahl, P. Skytt, J. Nordgren, and Y. Ma, Phys. Rev. B **49**, 1376 (1994).
[29] J.-H. Guo, S. M. Butorin, N. Wassdahl, P. Skytt, J. Nordgren, Y. Ma, P. Berastegut, and L.-G. Johansson, Phys. Rev. B **61**, 9140 (2000).
[30] P. Schroer, P. Kruger, and J. Pollmann, Phys. Rev. B **47**, 6971 (1993).
[31] A. Svane and O. Gunnarsson, Phys. Rev. Lett. **65**, 1148 (1990).
[32] A. Zunger and A. J. Freeman, Phys. Rev. B **16**, 2901 (1977).
[33] C. McGuinness, C. B. Stagarescu, P. J. Ryan, J. E. Downes, D. Fu, K. E. Smith, and R. G. Egdell, Phys. Rev. B **68**, 165104 (2003).